


RESEARCH PAPER



## LncRNA-GAS5 regulates PDCD4 expression and mediates myocardial infarction-induced cardiomyocytes apoptosis via targeting MiR-21

Xing-Hu Zhou<sup>a</sup>, Hong-Xia Chai<sup>b</sup>, Ming Bai<sup>a</sup>, and Zheng Zhang <sup>a</sup>

<sup>a</sup>Department of Cardiology, the First Hospital of Lanzhou University; Key Laboratory for Cardiovascular Diseases of Gansu Province, Lanzhou University, Lanzhou, P.R.China; <sup>b</sup>Department of Obstetrics and Gynecology, The First Hospital of Lanzhou University, Lanzhou, P.R.China

### ABSTRACT

The present study was designed to investigate whether and how lncRNA-GAS5 regulates cardiomyocyte apoptosis in MI. MI rat model was established by the left anterior descending (LAD) coronary artery ligation. MI model was further evaluated by biomarkers detection and TUNEL, HE and Masson staining. The roles of lncRNA-GAS5 on hypoxia/reoxygenation (H/R)-induced cardiomyocytes survival, cell cycle arrest, and apoptosis were examined by MTT and flow cytometry in rat heart-derived H9c2 cells. Western blot was used to determine the effect of GAS5 on the expression of apoptosis-associated proteins and PI3 K/AKT signaling pathway. The direct bindings of GAS5 to miR-21 and miR-21 to PDCD4 were measured by dual-luciferase reporter assay or RNA immunoprecipitation. Decreased expressions of GAS5 and PDCD4 as well as increased miR-21 level were observed in the hearts of MI-modeled rat, accompanying with morphologically myocardial cell injury, as well as collagen deposition and fibrosis, and elevated levels of cTnI, CK, CK-MB and LDH. In the cell model, the knockdown of GAS5 promoted cell survival, prevented cell cycle arrest and inhibited cell apoptosis while the overexpression of GAS5 showed the opposite effects. GAS5 was found to downregulate miR-21 and the effects of GAS5 were attenuated by miR-21 mimics. GAS5 positively regulated PDCD4 expression by functioning as a sponge of miR-21 in H/R model. Moreover, GAS5 stimulated PDCD4 and suppressed PI3 K/AKT signal pathway. LncRNA-GAS5 regulates PDCD4 expression to mediate MI-induced cardiomyocyte apoptosis via targeting miR-21, suggesting that GAS5 could be a therapeutic target for MI.

### ARTICLE HISTORY

Received 3 September 2019  
Revised 11 December 2019  
Accepted 11 March 2020

### KEYWORDS

Myocardial infarction;  
apoptosis; lncRNA-GAS5;  
miR-21; PDCD4

## Introduction

Myocardial infarction (MI) is the major cause of morbidity and mortality worldwide. The magnitude of MI determines left ventricular remodeling and heart failure. Current therapies for MI largely focus on antiplatelet and antithrombotic treatments and coronary anatomy where necessary [1]. Despite that, ischemic heart disease remains a major global cause of death and disability and alternative strategy is required. MI is accompanied with cardiomyocytes death during the acute ischemic stage and the loss of surviving cells during the subacute and chronic stages, which are mainly contributed from cardiomyocytes apoptosis [2]. In this case, cardiomyocytes are replaced with fibroblasts and fibrous tissue, which essentially regulate heart function and the development of heart failure and determine the size, shape, and wall thickness of ventricles [3–5]. Thus, the inhibition of cardiomyocytes apoptosis could be a promising therapeutic approach for the treatment of MI.

MicroRNAs (miRNAs) are small endogenous non-coding RNAs that regulate gene expression [6]. Mounting evidences show that miRNAs play roles in the regulation of various cancers and neurodegenerative disorders and the effects of miRNAs in the cardiac pathophysiology are increasingly appreciated [7,8]. MiR-21 is a well-known cardioprotective miRNA that promotes cardiac fibrotic remodeling and fibroblast proliferation [9,10]. MiR-21 was revealed to be up-regulated in the infarcted zone after MI and promote cardiac fibrosis *in vivo* [11]. Besides, it can target genes involved in cell growth, proliferation and apoptosis [12,13]. Programmed cell death 4 (PDCD4) is a tumor suppressor gene that modulates cell transformation, cell growth, and cell apoptosis [14–16]. MiR-21 can directly target PDCD4 [17,18] and negatively regulate PDCD4 expression [17].

Long non-coding RNAs (lncRNAs) are the transcripts longer than 200 nucleotides without

protein-coding capacity [19]. Recently, lncRNAs have been shown to be dysregulated in the heart failure. For example, lncRNA metastasis-associated lung adenocarcinoma transcript 1 (MALAT1) was highly expressed in MI process and promoted myocardial apoptosis through enhancing phosphatase and tensin homolog (PTEN) deleted on chromosome 10 expression by sponging miR-320 in mouse acute myocardial infarction (AMI) [20]. Moreover, hypoxia stimulated the expression of lncRNA THRIL and the inhibition of THRIL showed a protective effect against hypoxia-induced injuries by up-regulating miR-99a expression, suggesting the negative effect of THRIL in MI development [21]. The growth arrest-specific 5 (GAS5) is a single-strand non-coding RNA largely accumulated in growth-arrested cells [22]. It is involved in biological processes including cell growth arrest, cell proliferation, and apoptosis [23–25]. A previous study revealed a negative correlation between GAS5 and miR-21 [26]. However, whether and how lncRNA-GAS5 regulates cardiomyocytes apoptosis in MI process is unclear.

In the present study, we revealed that lncRNA-GAS5 was down-regulated in MI and promoted H/R-induced cardiomyocytes apoptosis by targeting miR-21. GAS5 positively regulated PDCD4 expression and negatively modulated phosphatidylinositol 3-kinases (PI3 K)/protein kinase B (AKT) signal pathway, suggesting that lncRNA-GAS5 could mediate MI-induced cardiomyocytes apoptosis via targeting miR-21-targeted PDCD4 and inactivating PI3 K/AKT signal pathway. Thus, lncRNA-GAS5 could be a potential target for the treatment of MI, the novel viewpoints obtained from the present research are of great importance to provide a supplemented thought for the prevention, treatment and prognosis of MI disease.

## Materials and methods

### Experimental animals and MI rat model

All animal experiments were compliant and approved by Animal Care and Ethics of the First Hospital of Lanzhou University. The left anterior descending (LAD) coronary artery ligation was performed to establish MI model as previously reported [27]. Briefly, rats were adaptively raised

for a week and randomly divided into two groups: MI group and sham group, followed by a modeling operation. In MI group, the rats primarily anesthetized with pentobarbital sodium were ventilated with a small ventilator and subjected to a left-sided thoracotomy. The LAD was encircled and ligated using a 7/0 silk suture. In addition, the sham-operated rats were treated similarly to the rats in MI group without ligation. The successful model was preliminarily determined with the left ventricular becoming white. During the experiments, there were 15 rats in each group, and among them, five rats were used to conduct the qPCR analysis and the others to perform the TTC staining and TUNEL staining, etc.

### 2,3,5-triphenyltetrazole chloride staining and terminal-deoxynucleotidyl transferase/(TdT)-mediated nick end labeling assay

After 3 or 7 days' ligation, the hearts were collected and fixed in 4% paraformaldehyde overnight for TTC staining according to a previous study [28]. In short, the heart tissues were cut into small pieces, which were further placed into the 2% of TTC staining solution. After incubation at 37°C for 30 min, the MI area was observed. Moreover, the apoptosis of cardiomyocytes in heart tissues was measured by the TUNEL assay using a detection kit (Roche, Basel, Switzerland) following the manufacturer's instruction. The heart sections were digested using the proteinase K solution for 15 min and then immersed in PBS, which next covered and immersed in a stop reagent for terminating the enzymatic reaction. Rinsing with PBS was used to treat the sections. The incubation with streptavidin-horseradish peroxidase solution was performed for 30 min in the condition without light. After washed, the slides were exposed to 3,3'-diaminobenzidine and hematoxylin. Lastly, the numbers of TUNEL positive and total cells were counted.

### Hematoxylin-eosin (HE) staining

The collected heart tissues from MI rats or sham rats were fixed by immersion of formalin. After a normative pruning, heart tissues mass was received the dehydration by gradient concentrations of

alcohol and hyalinization by dimethylbenzene. The tissues then were placed into the melted paraffin and cut into thin sections about 5  $\mu\text{m}$ . Also, they were dehydrated and hyalinized with the mentioned reagents above, respectively. Hematoxylin and eosin were successively stained the sections. After gum sealing, the heart tissue sections were observed under a light microscope.

### **Masson staining**

The pre-treatment of tissues were basically the same as the operation of HE staining. Next, the slices were stained with Bouin solution at room temperature overnight, and then rinsed with running water. Celestine blue staining solution was dripped to the slices for staining. After washed slightly, hematoxylin staining solution was next dripped for staining. Washed slightly, the acid ethanol differentiation solution was used, followed by a rinse with running water for 10 min. Lichunhong fuchsin staining solution and phosphomolybdic acid solution were used to treat the slices for 10 min, respectively. Then, they were stained with aniline blue dye for 5 min, prior to dehydration, hyalinization, neutral gum sealing. Finally, the morphology was observed under a light microscope.

### **Enzyme-linked immunosorbent assay (ELISA) assay**

The fresh blood from rats was harvested and centrifuged at the speed of 500 g for 10 min at 4°C for extracting the serum. The content of cardiac troponin I (cTnI) was determined using the ELISA kit (Abcam, Cambridge, MA, USA), according to the detailed introduction provided by the manufacturer. Briefly, after conducted the reaction with related reagents, the absorbance of each well was quantified by a microplate reader. At the same time, various standard cTnI reagents were used to build a standard curve under the same reaction condition. Then, the content of cTnI in each well was calculated according to the standard curve.

### **Biochemical detection**

The activities of creatine kinase (CK), lactate dehydrogenase (LDH) and creatine kinase-muscle/brain

(CK-MB) in rat serum were determined by the commercial CK and LDH detection kits (Solarbio, China) and CK-MB detection kit (Sigma-Aldrich, USA) according to the provided instructions. The detection methods were all based on the colorimetry.

### **Cell culture and *in vitro* H/R**

Rat heart-derived cells, H9c2 cell line, purchased from the American Type Culture Collection (ATCC, Rockville, MD, USA) were maintained in Dulbecco's modified Eagle's medium (DMEM) with supplemented with 10% fetal bovine serum and 1% penicillin/streptomycin. The H/R model of cells was established by inducing hypoxia as previously reported [29]. H9c2 cells were cultured in an anaerobic chamber maintained at 37°C with humidified atmosphere of 5% CO<sub>2</sub>, 10% H<sub>2</sub>, and 85% N<sub>2</sub> for the required time (4–20 h) followed by reoxygenation with the normal culture condition for 3 h.

### **Plasmid construct and transfection**

Rat GAS5, PTEN, and PDCD4 fragment was amplified using PCR and cloned into the psiCHECK-2 vector. Cloning of GAS5 with mutations at the putative miR-21 binding site was constructed using the Phusion™ site-directed mutagenesis kit (Thermo Fisher Scientific). For the measurement of luciferase activity, the prepared constructs were co-transfected with miR-21 mimics or negative control (NC) into H9c2 cells using Lipofectamine 2000 (Thermo Fisher Scientific) following the manufacturer's instruction. For the investigation of the effect of GAS5, miR-21 or PDCD4, cells were transfected with shGAS5, GAS5 over-expression vector (OE-GAS5), shPDCD4 or miR-21 mimics. The shGAS5, shPDCD4, miR-21 mimics and their negative control ones were synthesized by GenePharma (China, Suzhou).

### **Dual luciferase reporter assay**

The wild-type GAS5 (GAS5-WT), mutant GAS5 (GAS5-MUT), and wild-type or mutant of PDCD4-3'UTR were synthesized and subsequently load into pMIR-GLO™ Luciferase vectors (Promega, WI, USA). Cells were seeded into a 96-well plate. To demonstrate the relationship between GAS5 and miR-21, the vectors containing the GAS5-WT or

GAS5-MUT and miR-21 mimics or miR-NC were transfected into cells using Lipofectamine 2000 reagent. In addition, the vectors of PDCD4 plus miR-21 were also transfected to cells using Lipofectamine 2000 reagent to determine the correlation of PDCD4 and miR-21. At 48 h post-transfection, luciferase activities were determined using a Dual-Glo Luciferase Assay System (Promega) following the manufacturer's protocol. Firefly luciferase activity was normalized to Renilla luciferase activity. Luciferase activities were determined using the Dual-Luciferase Reporter Assay System.

### **RNA immunoprecipitation (RIP)**

RNA immunoprecipitation was performed using the Magna RIP RNA-Binding Protein Immunoprecipitation Kit according to the manufacturer's protocol (Millipore). Cell lysate was immunoprecipitated with IgG or AGO2 antibody (Cell Signaling Technology). After the antibody was recovered by protein A + G beads, qPCR was performed to detect GAS5 and miR-21 in the precipitates.

### **3-(4,5-dimethylthiazol-2-yl)-2,5-diphenyltetrazolium bromide (MTT) assay**

Cell survival was measured using the MTT assay according to the reported protocol with modification [30]. H9c2 cells were seeded into a 96-well plate with a density at  $1 \times 10^4$ /well. After appropriate treatments, MTT solution (5 mg/mL, in PBS) was added, followed by the incubation for 4 h. After removal of medium, dimethyl sulfoxide (DMSO) was added to dissolve the formed formazan crystal. The absorbance was measured at 490 nm.

### **Cell cycle assay**

The cell cycle phase distribution was assessed using flow cytometry. Cells were seeded into a 6-well plate at  $1 \times 10^6$  and transfected accordingly. After 36 h, cells were trypsinized and washed twice with ice-cold phosphate buffer saline (PBS) followed by centrifugation. Cell pellet was resuspended in 50  $\mu$ L of ice-cold PBS and 450  $\mu$ L

of ice-cold methanol for 1 h at 4°C followed by centrifugation, washing, and resuspension in PBS with RNAase (20  $\mu$ g/mL). After incubation at 37°C for 30 min, cells were chilled over ice for 10 min and stained with propidium iodide (PI) (50  $\mu$ g/mL) for 1 h. The analysis was performed using Calibur (BD Biosciences).

### **Cell apoptosis assay**

For the determination of cell apoptosis, cells were seeded into a 6-well plate at  $1 \times 10^6$ . After 48 h of transfection, cells were dissociated, washed, and resuspended in  $1 \times$  binding buffer (BD Biosciences). They were then stained with AnnexinV-fluorescein isothiocyanate (FITC) and PI by adding 5  $\mu$ L of each solution into 100  $\mu$ L of cell suspension according to the manufacturer's instruction (BD Biosciences). Following incubation at room temperature in the dark for 15 min, cell apoptosis was evaluated by fluorescence-activated cell sorting (FACS) analysis using Calibur (BD Biosciences).

### **Real-time quantitative polymerase chain reaction (qPCR)**

The fresh infarcted areas of myocardium and transfected cells were harvested for qPCR analysis. Total RNA was extracted by TRIzol reagent according to the introduction (Sigma-Aldrich, St. Louis, MO, USA). Reverse transcription was performed using random hexamer primer and MMLV Reverse Transcriptase (Promega). The qPCR for the quantification of gene transcripts was performed with  $2 \times$  HotStart SYBR Green qPCR Master Mix (TransGen Biotech) using a Stratagene Mx3000P (Agilent Technologies). The mRNA level was calculated relative to internal control using  $2^{-\Delta\Delta C_t}$  method using a real-time PCR system. The primers used in this study are as follows:

lncRNA-GAS5, forward:5'-ATCTGGTGGAA TCTCACAGGC-3', reverse: 5'- AGCTTGCCA TGCCTTCAGTTA-3';

miR-21, forward:5'-CGCGCTAGCTTATCAG ACTGA-3', reverse: 5'- CGGCCAGTGTTCAGACTAC-3';

PDCD4, forward:5'-AACGAAGTCGCGGAG ATGTT-3', reverse: 5'- TCTCGGAGTGTCAGGCTA-3';

PTEN, forward:5'-ATTCCCAGTCAGAGGCGCTA-3', reverse: 5'-TCACCTTTAGCTGGCA GACC-3';

U6, forward:5'-CTCGCTTCGGCAGCACA-3', reverse: 5'-AACGCTTCACGAATTTGCGT-3';

GAPDH, forward:5'-AGCCCAAGATGCCCTT CAGT-3', reverse: 5'-CCGTGTTCTACCCC CAATG A-3';

### Western blot

The transfected H9c2 cells were lysed with radio-immunoprecipitation assay (RIPA) buffer containing 0.01% protease and phosphatase inhibitors. The samples were then centrifuged at  $12,000 \times g$  for 15 min at 4°C and the supernatants were collected. The protein concentration in the supernatant was measured by a bicinchoninic acid (BCA) Protein Assay Kit (Thermo Fisher Scientific). Protein lysates were separated by 10% sodium dodecyl sulfate-polyacrylamide gel electrophoresis (SDS-PAGE) and transferred onto nitrocellulose membranes which were then blocked with 5% nonfat milk in t-butyltrimethylsilyl (TBS) containing 0.1% Tween-20 for 2 h at room temperature. Subsequently, membranes were incubated with relevant antibodies, anti-cleaved caspase-9 (1:1,000, Cell Signaling Technology), anti-B-cell lymphoma-2 (BCL-2) (1:1,000, Abcam), anti-BCL2-associated X protein (BAX) (1:1,000, Abcam), anti-PDCD4 (1:1,000, Abcam), anti-PI3 K (1:1,000, Abcam), anti-AKT (1:1,000, Cell Signaling Technology), anti-p-AKT (1:1,000, Cell Signaling Technology) and anti-glyceraldehyde-3-phosphate dehydrogenase (GAPDH) (1:1,000, Cell Signaling Technology) as a loading control at 4°C overnight. Following the incubation with horseradish peroxidase (HRP)-conjugated secondary antibody, membranes were incubated with ECL substrate and subjected for X-ray film exposure in the dark room.

### Statistical analysis

All data were presented as mean  $\pm$  standard deviation (SD) from at least three independent experiments. Data were analyzed by GraphPad Prism 6.0 (GraphPad Software Inc., San Diego, CA). Statistical differences were performed using unpaired two-tailed *t*-test for comparison between

two groups and one-way analysis of variance (ANOVA) followed by Tukey post hoc test for multiple comparison. The *p* value less than 0.05 was considered statistically significant. \*, *p* < 0.05; \*\*, *p* < 0.01; \*\*\*, *p* < 0.001.

## Results

### Decreased expression of GAS5, PDCD4 and PTEN and increased miR-21 level in tissues from MI model

The MI rat model was established using LAD coronary artery ligation. The TTC staining showed a larger infarcted zone with the white area in the heart in MI group than sham group with the time of 3 or 7 days (Figure 1(a)). TUNEL staining revealed more apoptotic cells in MI group (Figure 1(b,c)). At the level of morphology, myocardial cell injury, collagen deposition and fibrosis were observed in the MI animal model, and the morphological damage degree in 7 days was more severe than that in 3 days (Figure 1(d)). Moreover, we found elevated levels of cTnl, CK, CK-MB and LDH in the MI model (Figure 1(e,f)). Taken together, these suggested that the MI model was established more successfully after 7 days. Under this circumstance, the mRNA levels of GAS5, PDCD4, and PTEN were significantly decreased while miR-21 largely was induced in the rat after MI compared to the sham group (Figure 1(g)). All these suggested that MI can cause cardiomyocytes apoptosis, suppress GAS5, PDCD4, and PTEN expression, and elevate miR-21 level.

### LncRNA GAS5 regulates H/R-induced cardiomyocytes proliferation and apoptosis

The cell model was established by inducing hypoxia for 4–20 h followed by reoxygenation for 3 h in H9c2 cells cultured without glucose. Data showed that hypoxia induced the decrease of GAS5, PDCD4, and PTEN expression and increased miR-21 level in a time-dependent manner with maximum effect at 16 h (Figure 2(a)). Hypoxia for 16 h followed by reoxygenation for 3 h was then used throughout the following experiments. To investigate the effect of GAS5 on cardiomyocytes apoptosis, the vectors of overexpression GAS5 (OE-GAS5) and shGAS5

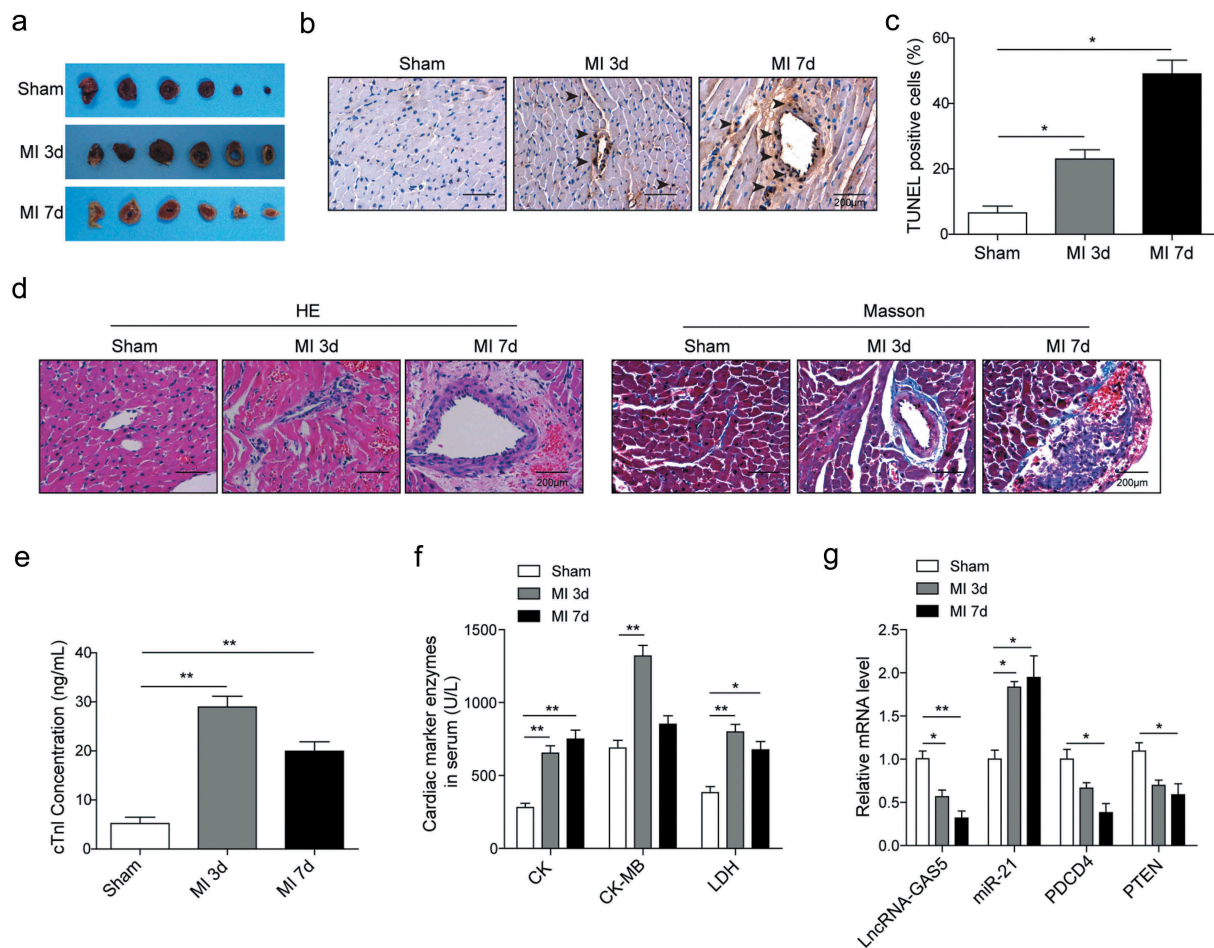


**Figure 1.** Decreased expression of GAS5, PDCD4 and PTEN and increased miR-21 level in tissues from MI model. (a) The representative images of TTC staining of sham- or MI-treated rat heart tissues. (b and c) The TUNEL assay of the tissue apoptosis in the rat heart. (d) The images of HE staining and Masson staining of sham- or MI-treated rat heart tissues. (e) ELISA detection of cTnI content in sham- or MI-treated rat serum. (f) The activities analysis of CK, CK-MB and LDH in sham- or MI-treated rat serum. (g) The expression levels of lncRNA-GAS5, miR-21, PDCD4 and PTEN in sham- or MI-treated rat heart tissues. \* $p < 0.05$  and \*\* $p < 0.01$ .

plasmids were made and transfected into H9c2 cells. The results showed the successful overexpression or knockdown GAS5 in H9c2 cells (Figure 2(b)). MTT assay was performed to determine the effect of GAS5 on cell survival in both sham and H/R groups. Data presented that the overexpression or knockdown of GAS5 did not significantly change the survival rate in sham-treated cells (Figure 2(c)). However, the reduction of GAS5 level promoted but overexpression GAS5 decreased the survival rate of H/R-treated cells (Figure 2(c)). Flow cytometry assay was further performed to investigate the role of GAS5 on cell cycle. It was found that the overexpression of GAS5 arrested the cell cycle at G1 phase (Figure 2(d)). Cell apoptosis was then measured and data demonstrated that the overexpression of GAS5 promoted cell apoptosis while the knockdown showed the opposite

effect (Figure 2(e)). Moreover, the GAS5 overexpression caused increased expression of cleaved caspase-9 and BAX but reduced BCL-2 expression. Inversely, knockdown of GAS5 suppressed cleaved caspase-9 and BAX level but promoted BCL-2 expression (figure 2(f)).

### **LncRNA GAS5 directly targets miR-21**

To verify whether miR-21 is the direct target of GAS5, the starbase (<http://starbase.sysu.edu.cn/>) and targetscan (<http://www.targetscan.org/>) are performed to predict the binding site (Figure 3(a)). H9c2 cells were transfected with control miR (miR-NC) or miR-21 mimics followed by the introduction of GAS5-WT or GAS5-MUT dual luciferase reporter plasmid. Data of dual luciferase reporter assay

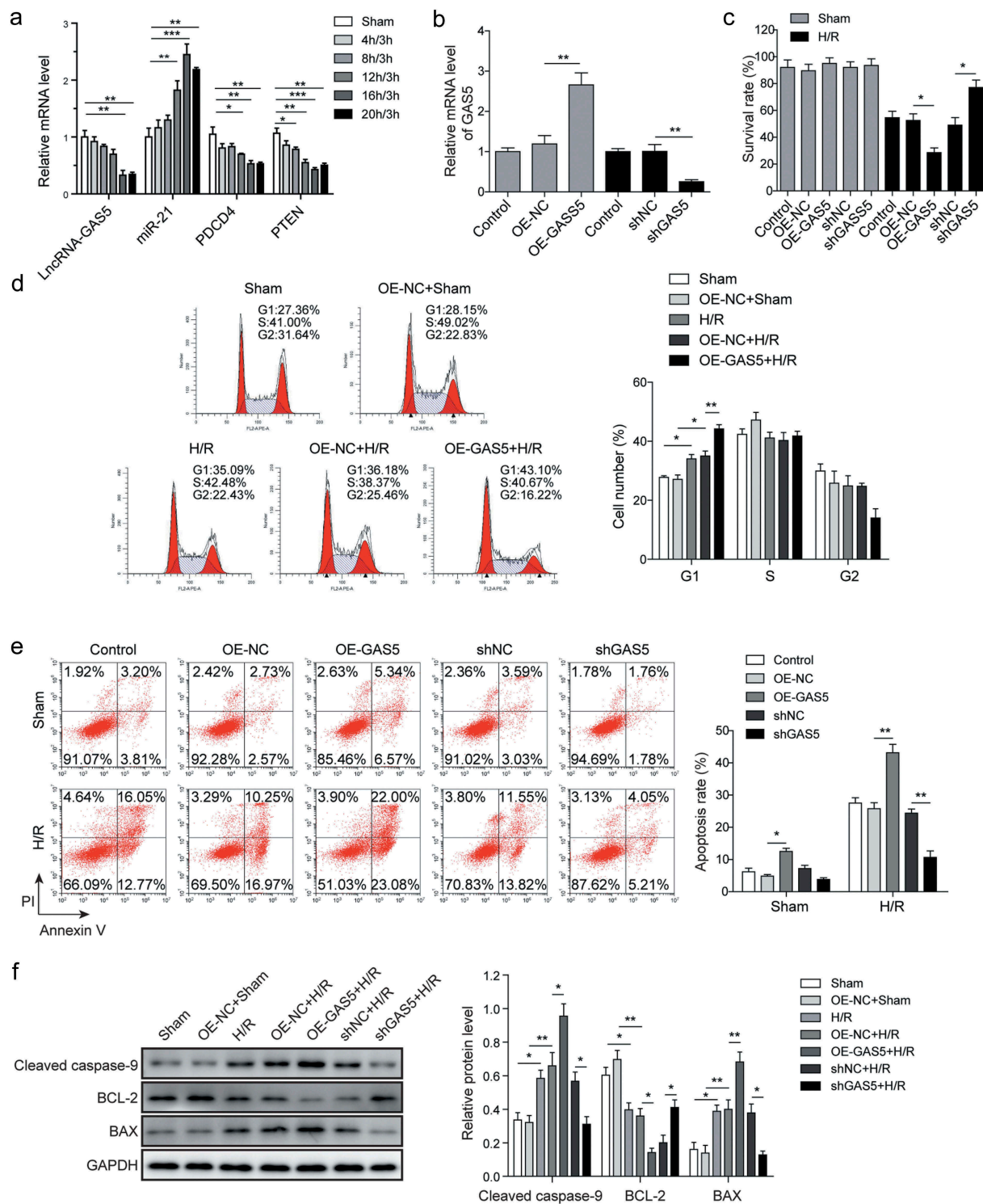


**Figure 2.** GAS5 regulates H/R-induced cardiomyocyte proliferation and apoptosis. (a) The qPCR analysis of expressions of lncRNA-GAS5, miR-21, PDCD4 and PTEN in H9c2 cells induced by hypoxia for 4–20 h followed by reoxygenation for 3 h. (b) The qPCR analysis of lncRNA-GAS5 expression after overexpression of GAS5 (OE-GAS5) or knockdown of GAS5 (shGAS5). (c) Cell survival assessed by MTT method in H9c2 cells. (d) Cell cycle detection by flow cytometry. (e) Cell apoptosis analysis by flow cytometry under different conditions. (f) Representative images of western blot showing the protein expressions of cleaved caspase-9, BCL-2 and BAX in the cells under different conditions. GAPDH was used as a loading control. Data are presented as the mean  $\pm$  SD from at least three independent experiments. OE-GAS5: overexpression of GAS5; OE-NC: overexpression of empty plasmid; shGAS5: knockdown of GAS5 with shRNA; shNC: shRNA negative control. \* $P < 0.05$ , \*\* $P < 0.01$  and \*\*\* $P < 0.001$ .

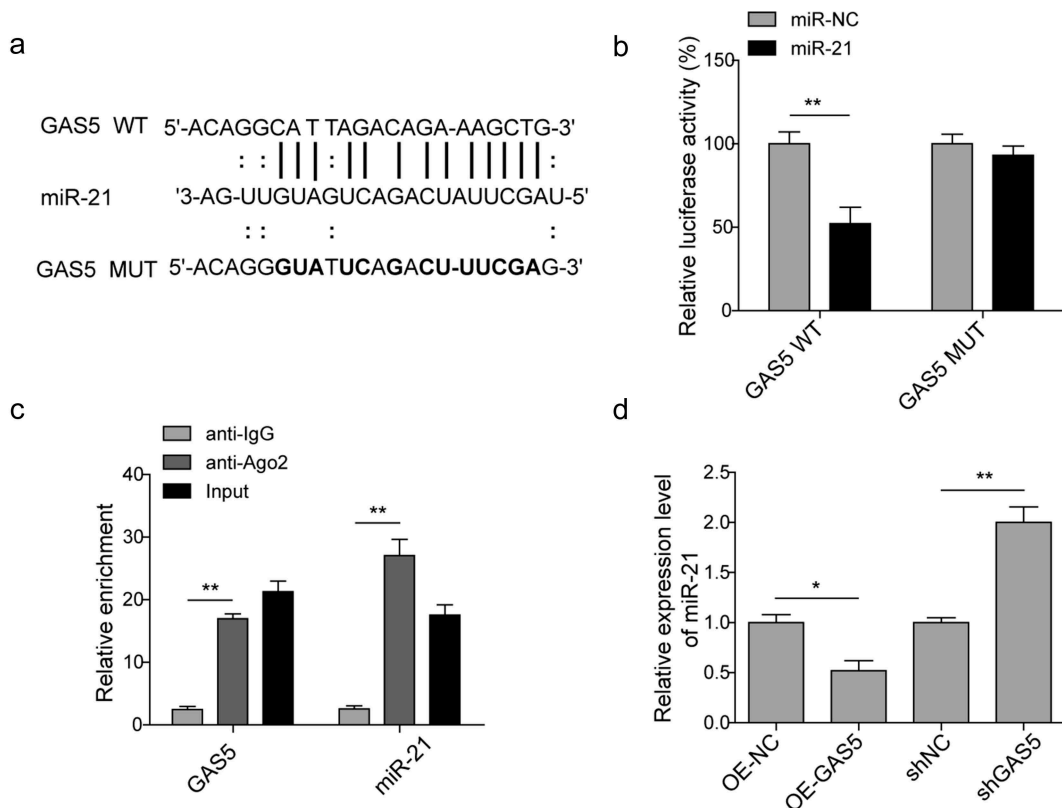


**Figure 3.** LncRNA GAS5 directly targets miR-21. (a) MiR-21 binding sites in the lncRNA GAS5. Thirteen nucleotides (bold mutated in luciferase reporter plasmids carrying GAS5). (b) Dual luciferase reporter assay in H9c2 cells transfected with miR-NC or miR-21 mimics followed by the introduction of GAS5-WT or GAS5-MUT. (c) RIP analysis of GAS5 and miR-21 immunoprecipitated by anti-Ago2. The anti-IgG as a negative control. (d) The qPCR analysis of miR-21 level in the cells transfected with OE-GAS5 or shGAS5. Data are presented as the mean  $\pm$  SD from at least three independent experiments. OE-GAS5: overexpression of GAS5; OE-NC: overexpression of empty plasmid; shGAS5: knockdown of GAS5 with shRNA; shNC: shRNA negative control. \* $p < 0.05$  and \*\* $p < 0.01$ .

revealed that miR-21 mimics inhibited the luciferase activities of GAS5-WT but not GAS5-MUT (Figure 3(b)), suggesting that GAS5 can target miR-21. Since AGO2 is a key component of the RNA-induced silencing complex (RISC), connecting miRNAs and their binding sites for mRNA. The associated miRNA and mRNA can be obtained by the proper immunoprecipitation of AGO2. The RIP of AGO2 was performed here and the data showed that GAS5 and miR-21 were enriched in the AGO2 pellet (Figure 3(c)). The effect of GAS5 on the expression of miR-21 was then determined by either overexpression or knockdown of GAS5. The qPCR results presented that the overexpression of GAS5 induced the reduction of miR-21 level, while the knockdown of GAS5 generated the opposite effect (Figure 3(d)). Taken these results, GAS5 can directly regulate miR-21 in H9c2 cells.

### **MiR-21 is involved in the cardiomyocytes apoptosis inducing by lncRNAGAS5**

We then determined whether GAS5 could regulate the survival of H/R-induced cardiomyocytes via targeting miR-21. The results of MTT showed that miR-21 mimics increased cell survival and the effect of GAS5 on decreasing cell survival was reversed by the miR-21 mimics (Figure 4(a)). Consistent with the data in Figure 2, on the contrary to miR-21 mimics, GAS5 overexpression arrested cell cycle, which was attenuated by the co-transfection with miR-21 mimics. Moreover, GAS5 repressed miR-21-mediated cell cycle promotion (Figure 4(b)). Furthermore, miR-21 mimics inhibited cell apoptosis while the overexpression of GAS5 facilitated cell apoptosis, which was also reduced by the co-transfection with miR-21 mimics (Figure 4(c)). The role of GAS5 and miR-21 on the



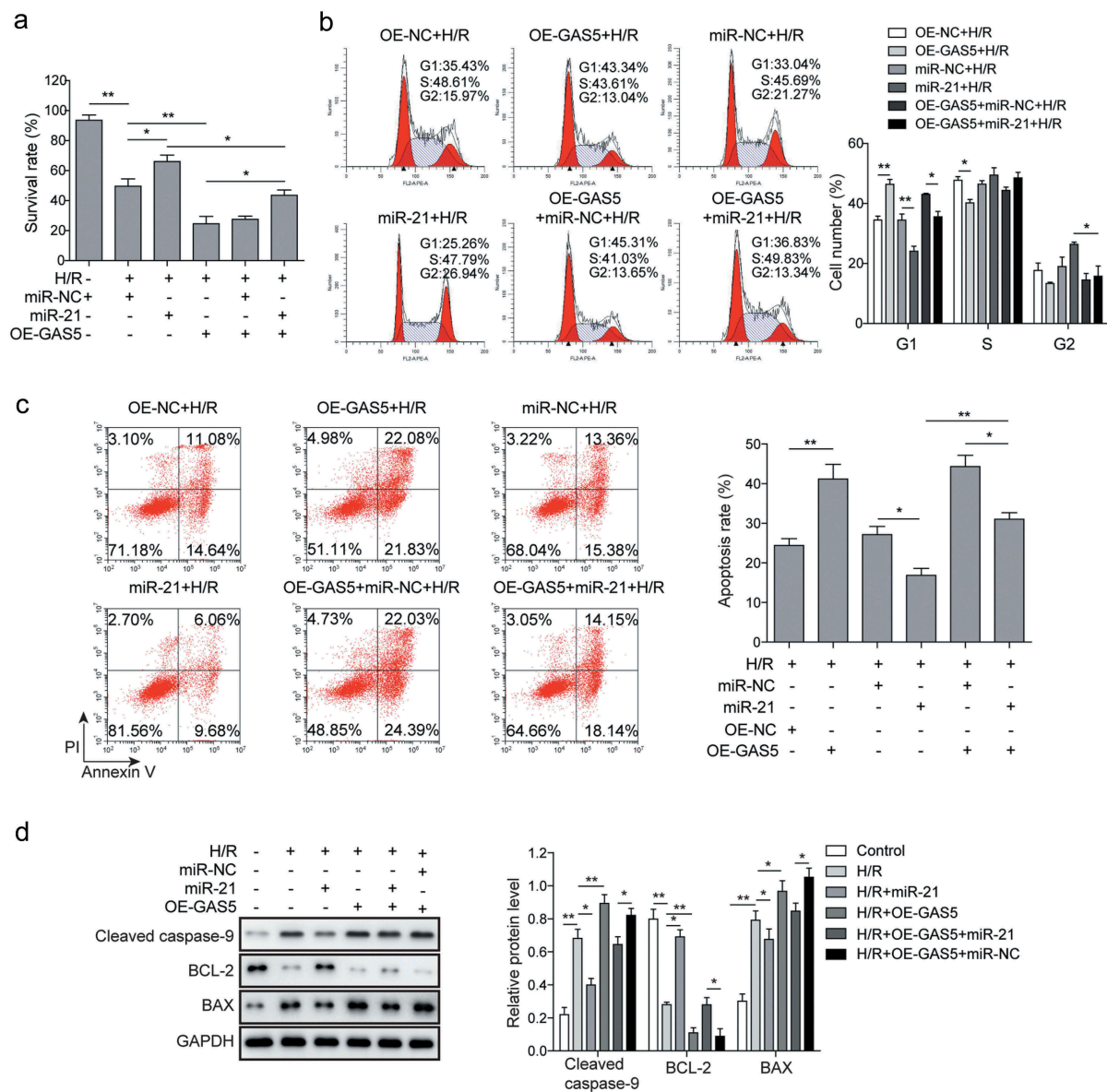


**Figure 4.** MiR-21 is involved in cardiomyocytes apoptosis induced by lncRNA GAS5. (a) MTT measurement in control or H/R (16 h/3 h)-treated H9c2 cells transfected with miR-21 mimics or GAS5 or co-transfected with miR-NC or miR-21 and GAS5. (b) Cell cycle determination by flow cytometry in the cells treated with OE-NC+H/R, OE-GAS5 + H/R, miR-NC+H/R, miR-21 + H/R, OE-GAS5+ miR-NC+H/R, OE-GAS5+ miR-21 + H/R. (c) Cell apoptosis analysis by flow cytometry in the cells treated with OE-NC+H/R, OE-GAS5 + H/R, miR-NC+H/R, miR-21 + H/R, OE-GAS5+ miR-NC+H/R and OE-GAS5+ miR-21 + H/R. (d) Western blot showing the protein expression of cleaved caspase-9, BCL-2, and BAX in the cells transfected with miR-21 mimics or GAS5 or co-transfected with miR-NC or miR-21 and GAS5 under H/R (16 h/3 h). GAPDH was used as a loading control. Data are presented as the mean $\pm$ SD from at least three independent experiments. OE-GAS5: overexpression of GAS5; OE-NC: overexpression of empty plasmid; \* $p < 0.05$  and \*\* $p < 0.01$ .

expression of cell apoptosis-associated proteins was then measured and the results presented that the expression of BCL-2 was promoted, while the level of cleaved caspase-9 and BAX were attenuated by miR-21 mimics. GAS5 overexpression stimulated cleaved caspase-9 and BAX expression but suppressed

BCL-2 expression. Further, the effect of miR-21 mimics on the apoptosis-associated proteins expression was partially recovered by GAS5 overexpression (Figure 4(d)). All these data illustrated that GAS5 could induce H/R-mediated cardiomyocytes apoptosis partly via miR-21.

### **LncRNA GAS5 positively regulates PDCD4 expression by functioning as a sponge of miR-21 in H/R**

It was reported that PDCD4 was one of the potential targets of miR-21. We further investigated the role of miR-21 on the expression of PDCD4. Dual luciferase reporter assay showed that miR-21 mimics significantly inhibited the activities of wild type of PDCD4 3'UTR while it showed little effect on PDCD4-MUT (Figure 5(a)), suggesting that miR-21 targeting PDCD4 in H9c2 cells under H/R condition. Moreover, the introduction of miR-21 mimics reduced PDCD4 expression. The overexpression of GAS5 attenuated the reduction effect of miR-21 and shPDCD4 on PDCD4 expression (Figure 5(b,d)). In addition, GAS5 knockdown could inhibit the expression of PDCD4 (Figure 5(e)). Furthermore, the knockdown of PDCD4 repressed cell apoptosis and attenuated GAS5 overexpression-induced cell apoptosis (figure 5(f)). Meanwhile, PDCD4 knockdown significantly inhibited the expression of cleaved caspase-9 and BAX but stimulated BCL-2 expression and reduced the effects induced by GAS5 overexpression on expressions of above apoptosis proteins (Figure 5(g)).

### **LncRNAGAS5 positively regulates PDCD4 and suppresses PI3 K/AKT signal pathway**

PDCD4 was revealed to regulate PI3 K/AKT signal pathway which is a key signal pathway regulating cell survival and apoptosis [31]. The effect of GAS5 on PDCD4-mediated PI3 K/AKT signal pathway was further demonstrated. It was shown that the expression levels of PI3 K and phosphorylated AKT (p-AKT) in cardiomyocytes of H/R was inhibited by GAS5 overexpression, but up-regulated by miR-21 mimics or shPDCD4. In addition, miR-21 mimics or shPDCD4 attenuated GAS5 overexpression-induced inhibition of PI3 K and p-AKT expression. Meanwhile, AKT inhibitor (Palomid 529) also partially rescued the effect of shPDCD4 on the PI3 K/AKT signal pathway (Figure 6(a,b)). Moreover, we also added Palomid 529 to the shPDCD4 or miR-21 mimics treatment groups separately to validate the regulatory role of PDCD4 or miR-21 on PI3 K/AKT signal pathway. Figure 6(c,d) showed that the protein levels of

PI3 K and p-AKT in cardiomyocytes of H/R were promoted by miR-21 mimics or PDCD4 knockdown. Meanwhile, AKT inhibitor can partially rescue the effect of miR-21 mimics or shPDCD4. Taken together, these results indicated that GAS5 inactivated PI3 K/AKT signal pathway through targeting miR-21/PDCD4 axis.

## **Discussion**

MI is one of the leading causes of death and disability worldwide, despite much-achieved advance of its management. Cardiomyocyte apoptosis induces progressive cardiomyocyte loss and the inhibition of cardiomyocyte apoptosis shows a beneficial effect on post-MI cardiac dysfunction [32,33]. So, exploration of the action of interactive molecules such as lncRNA, miRNA and mRNA, etc., regulating the apoptosis in cardiomyocytes is beneficial to develop new drugs or therapy method for MI treatment. The miR-21 plays a critical role in cardiomyocytes apoptosis in MI process and GAS5 is known to target miR-21. However, the effect of lncRNA-GAS5 on cardiomyocytes apoptosis in MI process is unclear. The present study demonstrated that GAS5 and PDCD4 were down-regulated while miR-21 was up-regulated in an *in vivo* model and *in vitro* model of H/R and GAS5 promoted PDCD4 expression and regulated MI-induced cardiomyocytes apoptosis via targeting miR-21.

The cTnl, CK, CK-MB and LDH were the biomarkers of MI [34]. Based on the alterations of morphological characteristics and indicated biomarkers, we confirmed the rat MI model was built successfully and the apoptosis was more significant after 7 days. As illustrated in a published work, PTEN was demonstrated to participate in the process of MI [35]. Yuan et al. confirmed a conclusion regarding promotion of miR-21 to the cardiac fibrosis in MI process [11]. Similarly, we observed an elevated miR-21 expression level, and the low levels of PTEN and another apoptosis-regulated molecule PDCD4 in the tissues samples of MI. Different expression patterns of various lncRNAs has been found in MI patients compared to the healthy, showing its predictive value in the diagnosis of MI [36]. In the current study, GAS5 was found to express at a low level in MI rats.

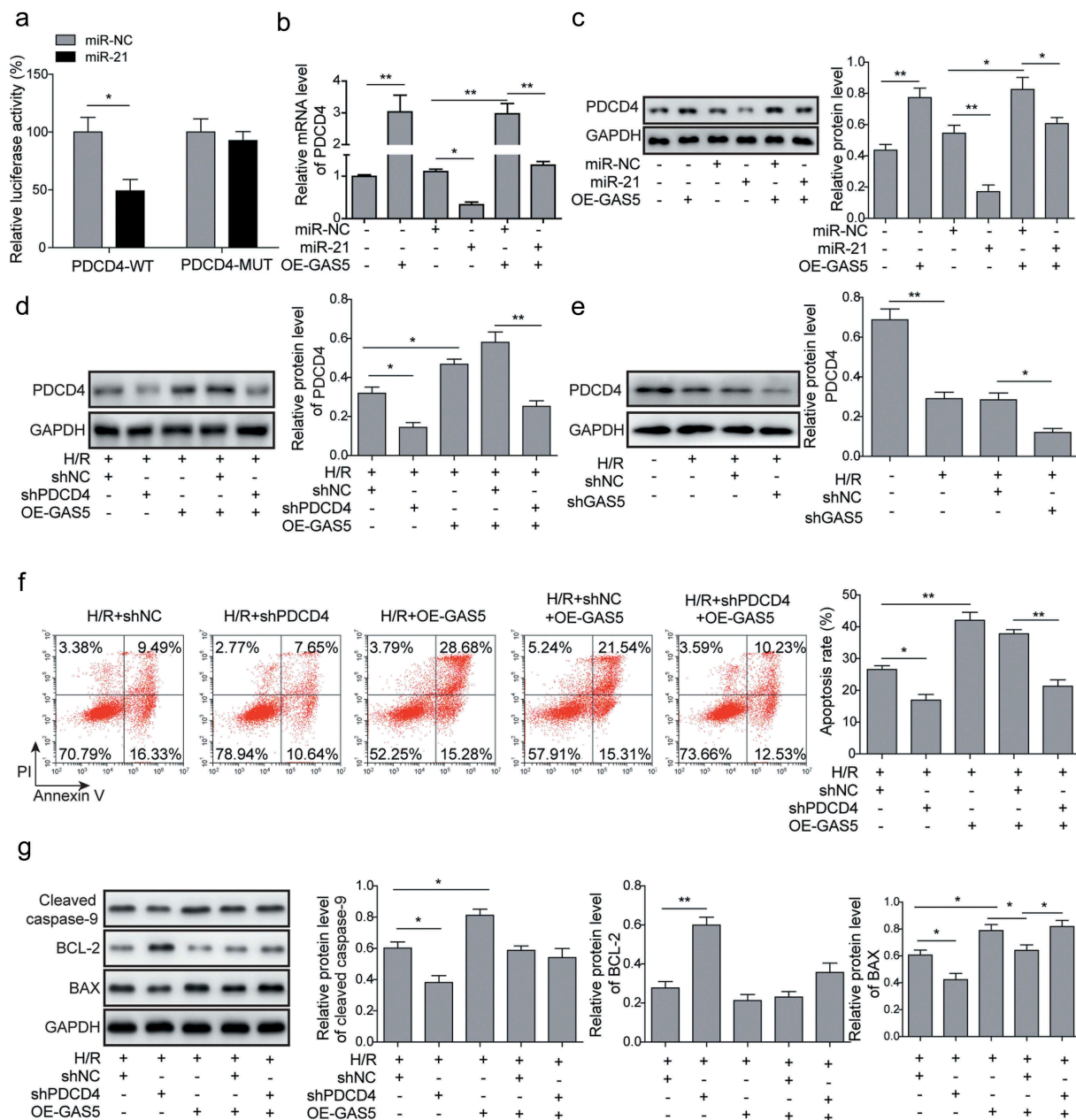


**Figure 5.** LncRNA GAS5 positively regulates PDCD4 expression by functioning as a sponge of miR-21 in H/R. (a) Dual luciferase reporter assay in the cells transfected with miR-NC or miR-21 and luciferase reporter plasmids carrying 3'-UTR of PDCD4. (b) qPCR analysis of PDCD4 in the cells transfected with GAS5, miR-NC, miR-21 mimics or co-transfected with miR-NC or miR-21 mimics and GAS5 under H/R (16 h/3 h). (c) Western blot showing the protein level of PDCD4 in the cells transfected with GAS5, miR-NC, miR-21 mimics or co-transfected with miR-NC or miR-21 mimics and GAS5 under H/R (16 h/3 h). (d) Western blot was applied to detect the protein level of PDCD4 in the cells transfected with shPDCD4 or GAS5 or co-transfected with shNC or shPDCD4 and GAS5 under H/R (16 h/3 h). (e) Western blot was applied to detect the protein level of PDCD4 in the cells of control, H/R, H/R+ shNC or H/R+ shGAS5 groups. (f) Measurement of cell apoptosis by flow cytometry in the cells transfected with shPDCD4 or GAS5 or co-transfected with shNC or shPDCD4 and GAS5 under H/R (16 h/3 h). (g) Western blot showing the protein expression of cleaved caspase-9, BCL-2, and BAX in the cells under H/R (16 h/3 h). Data are presented as the mean  $\pm$  SD from at least three independent experiments. \* $p < 0.05$  and \*\* $p < 0.01$ .

Expectedly, under the condition of H/R model, the *in vitro* experiments exhibited the same alteration trends in GAS5, miR-21, PDCD4 and PTEN, in comparison with the rat model, which was in

a hypoxia-challenged time-dependent manner. MI induces cardiac cell death which is mainly contributed from cell apoptosis. Here, cellular experiments revealed that the overexpression of

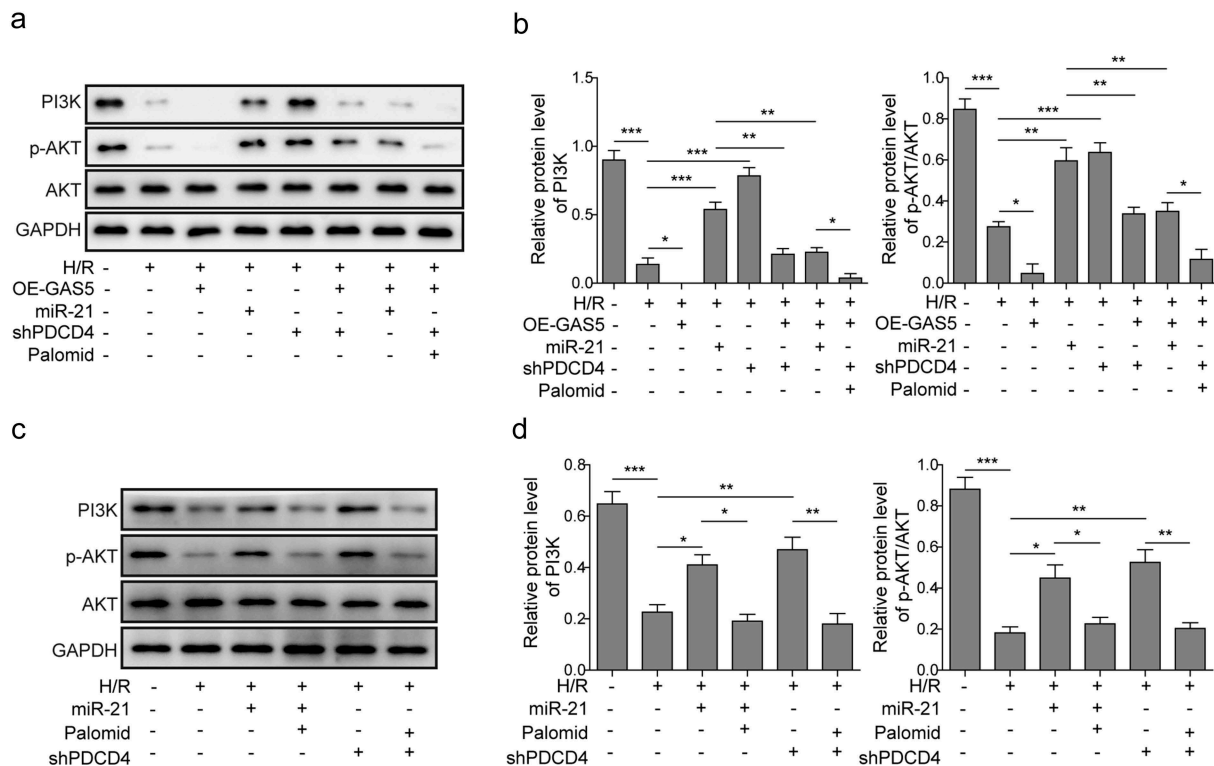


**Figure 6.** LncRNAGAS5 positively regulates PDCD4 and suppresses PI3 K/AKT signal pathway. (a) Representative image of western blot presenting the protein expression of PI3 K, p-AKT, and AKT in control or H/R(16 h/3 h)-treated cells induced by miR-21 mimics, OE-GAS5, or shPDCD4 or co-transfected by OE-GAS5 and miR-21 or shPDCD4 without or with the AKT inhibitor (Palomid, 2  $\mu$ M). (b) Densitometry performed for quantification of western blot. GAPDH was used as a loading control. (c) Representative image of western blot presenting the protein expression of PI3 K, p-AKT, and AKT in control or H/R-treated cells induced by miR-21 mimics or shPDCD4 without or with the AKT inhibitor (Palomid, 2  $\mu$ M). (d) Densitometry performed for quantification of western blot. GAPDH was used as a loading control. Data are presented as the mean  $\pm$  SD from at least three independent experiments. \* $P$  < 0.05, \*\* $P$  < 0.01 and \*\*\* $P$  < 0.001.

GAS5 arrested cell cycle and promoted cell apoptosis while the knockdown of it showed the opposite effect. The function of GAS5 on the promotion of cell apoptosis has been widely studied on various cancer cells including colorectal cancer cells, breast cancer cells, and bladder cancer cells [37–39]. However, it was also reported that GAS5 inhibited the apoptosis of cultured female germline stem cells [40]. These suggested that the function of GAS5 on apoptosis could dependent on cell type and disease conditions. Furthermore, Bax belongs to pro-apoptotic Bcl-2 family proteins and induces cytochrome *c* release and caspase activation, leading to cell apoptosis [41,42]. Bcl-2 could suppress Bax-induced apoptosis [41]. It was reported that Bcl-2 family proteins were involved in the modulation of cardiomyocyte apoptosis [43]. Here, we found the high expression level of GAS5 interfered with the balance between pro-apoptotic proteins, cleaved caspase-9 and Bax,

and anti-apoptotic protein Bcl-2, thereby determining cardiomyocytes apoptosis. Thus, GAS5 could contribute to the post-MI pathological process and might be a diagnostic or prognostic biomarker for MI.

The miR-21, an abundant miRNA in cardiomyocytes, shows a cardioprotective effect in MI process [44], while the underlying mechanism is less clear. Studies showed that miR-21 could functionally interact with lncRNAs. For example, lncRNA BISPR stimulated progression of thyroid papillary carcinoma by regulating miR-21-5p and lncRNA MEG3 suppressed proliferation of chronic myeloid leukemia cells by sponging miR-21 [45]. It was previously demonstrated that GAS5 and miR-21 formed a reciprocal repression feedback loop and GAS5 negatively regulated miR-21 expression through the RISC [26]. Moreover, GAS5 regulated proliferation and apoptosis in the growth plate by modulating fibroblast growth factor 1 (FGF1) expression via

mediating miR-21 [46]. In addition to heart disorders, the interaction of GAS5 and miR-21 has been found in osteoarthritis, atherosclerosis and cancer, etc. [47–49]. Here we also consistently observed the direct association between GAS5 and miR-21 in H/R model. Additionally, miR-21 reversed the effects of GAS5 on cell survival, cell cycle arrest, and cell apoptosis, presenting GAS5 regulated cardiomyocytes apoptosis in MI process via targeting miR-21.

PDCD4, a tumor suppressor gene, inhibits cell transformation, cell growth, and cell apoptosis. The mechanism-explored study revealed the possible inhibitory effect of PDCD4 on PI3 K/AKT/mTOR which is a key signal pathway regulating cell survival and apoptosis [31]. A previous study indicated that miR-21 negatively regulated PDCD4 [17]. We consistently observed that miR-21 directly targeted PDCD4 in H9c2 cells and down-regulated its expression in H/R model and therefore GAS5 positively modulated PDCD4 expression via targeting miR-21. Moreover, the apoptosis-related regulator PDCD4 was successively controlled by the GAS5 and miR-21 and the apoptosis alteration in H9c2 cells was in accordance with the changes in the expression of PDCD4 modulated by GAS5 and miR-21, which could be evaluated by the differential levels of anti-apoptosis protein Bcl-2 as well as pro-apoptosis proteins Bax and cleaved caspase-9. Importantly, the tight association among GAS5, miR-21 and PDCD4 were evidently demonstrated in other disorders including atherosclerosis and cancer [48,50]. It was well known that PTEN/PI3 K/AKT pathway could be affected by the miR-21 in pathological processes [51]. The PI3 K/AKT and several crucial proteins such as Bax, cleaved caspase-3 and cleaved caspase-9 form a pathway to exert pro- or anti-apoptosis effect [52]. Also, the miR-21 could directly act on the downstream PDCD4 for playing a crucial role in the cell apoptosis [53]. We concluded in this research that PDCD4 modulated PTEN to subsequently interfere with the PI3 K/AKT pathway in H/R model. The stimulation of PI3 K and p-AKT expression by GAS5 was suppressed by AKT inhibitor, suggesting that GAS5 regulated cardiomyocyte apoptosis via PDCD4-mediated PI3 K/AKT signal pathway. Interestingly, in H/R-based cell model, the relative PI3 K levels of H9c2 cells treated with shPDCD4 were higher than that with miR-21 over-expression, and the same result was not exhibited in

p-AKT expression level. Moreover, a recent study demonstrated that miR-21 regulated PI3 K/AKT/mTOR signaling by targeting transforming growth factor- $\beta$ 1 (TGF- $\beta$ 1) during skeletal muscle development [54]. Whether GAS5 regulates PI3 K/AKT/mTOR signal pathway through the modulation of TGF- $\beta$ 1 is unknown but worth investigation.

## Conclusions

To sum up, the present study demonstrated that the lncRNA-GAS5 is downregulated in MI and overexpression of it promotes PDCD4 expression and mediates MI-induced cardiomyocyte apoptosis via targeting miR-21, suggesting that GAS5 could be a potential diagnostic biomarker and a beneficial therapeutic target for MI.

## Acknowledgments

We would like to give our sincere gratitude to the reviewers for their constructive comments.

## Disclosure statement

The authors declare that they have no conflict of interest.

## Funding

This research did not receive any specific grant from funding agencies in the public, commercial, or not-for-profit sectors.

## ORCID

Zheng Zhang  <http://orcid.org/0000-0002-1819-7441>

## Data availability statement

All data generated or analyzed during this study are included in this published article.

## References

- [1] Spath NB, Mills NL, Cruden NL. Novel cardioprotective and regenerative therapies in acute myocardial infarction: a review of recent and ongoing clinical trials. *Future Cardiol.* 2016;12(6):655–672.
- [2] Takemura G, Fujiwara H. Role of apoptosis in remodeling after myocardial infarction. *Pharmacol Ther.* 2004;104(1):1–16.

- [3] Raïskina ME. Dynamics of the pathological changes in the heart during the acute stage of experimental myocardial infarct. *Kardiologija*. 1967;7(8):3–13.
- [4] Uusimaa P, Risteli J, Niemelä M, et al. Collagen scar formation after acute myocardial infarction: relationships to infarct size, left ventricular function, and coronary artery patency. *Circulation*. 1997;96(8):2565–2572.
- [5] Prabhu SD, Frangogiannis NG. The biological basis for cardiac repair after myocardial infarction: from inflammation to fibrosis. *Circ Res*. 2016;119(1):91–112.
- [6] Bartel DP. MicroRNAs: genomics, biogenesis, mechanism, and function. *Cell*. 2004;116(2):281–297.
- [7] Cheng Y, Ji R, Yue J, et al. MicroRNAs are aberrantly expressed in hypertrophic heart: do they play a role in cardiac hypertrophy? *Am J Pathol*. 2007;170(6):1831–1840.
- [8] van Rooij E, Sutherland LB, Liu N, et al. A signature pattern of stress-responsive microRNAs that can evoke cardiac hypertrophy and heart failure. *Proc Natl Acad Sci U S A*. 2006;103(48):18255–18260.
- [9] Cao W, Shi P, Ge JJ. miR-21 enhances cardiac fibrotic remodeling and fibroblast proliferation via CADM1/STAT3 pathway. *BMC Cardiovasc Disord*. 2017;17(1):88.
- [10] Cavarretta E, Condorelli G. miR-21 and cardiac fibrosis: another brick in the wall? *Eur Heart J*. 2015;36(32):2139–2141.
- [11] Yuan J, Chen H, Ge D, et al. Mir-21 promotes cardiac fibrosis after myocardial infarction via targeting Smad7. *Cell Physiol Biochem*. 2017;42(6):2207–2219.†.
- [12] Chan JA, Krichevsky AM, Kosik KS. MicroRNA-21 is an antiapoptotic factor in human glioblastoma cells. *Cancer Res*. 2005;65(14):6029–6033.
- [13] Si ML, Zhu S, Wu H, et al. miR-21-mediated tumor growth. *Oncogene*. 2007;26(19):2799–2803.
- [14] Wang Q, Sun Z, Yang HS. Downregulation of tumor suppressor Pdc4 promotes invasion and activates both beta-catenin/Tcf and AP-1-dependent transcription in colon carcinoma cells. *Oncogene*. 2008;27(11):1527–1535.
- [15] Zhen Y, Liu Z, Yang H, et al. Tumor suppressor PDCD4 modulates miR-184-mediated direct suppression of C-MYC and BCL2 blocking cell growth and survival in nasopharyngeal carcinoma. *Cell Death Dis*. 2013;4:e872.
- [16] Afonja O, Juste D, Das S, et al. Induction of PDCD4 tumor suppressor gene expression by RAR agonists, antiestrogen and HER-2/neu antagonist in breast cancer cells. Evidence for a role in apoptosis. *Oncogene*. 2004;23(49):8135–8145.
- [17] Asangani IA, Rasheed SAK, Nikolova DA, et al. MicroRNA-21 (miR-21) post-transcriptionally downregulates tumor suppressor Pdc4 and stimulates invasion, intravasation and metastasis in colorectal cancer. *Oncogene*. 2008;27(15):2128–2136.
- [18] Lu Z, Liu M, Stribinskis V, et al. MicroRNA-21 promotes cell transformation by targeting the programmed cell death 4 gene. *Oncogene*. 2008;27(31):4373–4379.
- [19] Peng JC, Shen J, Ran ZH. Transcribed ultraconserved region in human cancers. *RNA Biol*. 2013;10(12):1771–1777.
- [20] Hu H, Wu J, Li D, et al. Knockdown of lncRNA MALAT1 attenuates acute myocardial infarction through miR-320-Pten axis. *Biomed Pharmacother*. 2018;106:738–746.
- [21] Xia J, Jiang N, Li Y, et al. The long noncoding RNA THRIL knockdown protects hypoxia-induced injuries of H9C2 cells through regulating miR-99a. *Cardiol J*. 2018;26(5):564–574.
- [22] Schneider C, King RM, Philipson L. Genes specifically expressed at growth arrest of mammalian cells. *Cell*. 1988;54(6):787–793.
- [23] Kino T, Hurt DE, Ichijo T, et al. Noncoding RNA gas5 is a growth arrest- and starvation-associated repressor of the glucocorticoid receptor. *Sci Signal*. 2010;3(107):ra8.
- [24] Williams GT, Mourada-Maarabouni M, Farzaneh F. A critical role for non-coding RNA GAS5 in growth arrest and rapamycin inhibition in human T-lymphocytes. *Biochem Soc Trans*. 2011;39(2):482–486.
- [25] Wang YN, Shan K, Yao M-D, et al. Long noncoding RNA-GAS5: a novel regulator of hypertension-induced vascular remodeling. *Hypertension*. 2016;68(3):736–748.
- [26] Zhang Z, Zhu Z, Watabe K, et al. Negative regulation of lncRNA GAS5 by miR-21. *Cell Death Differ*. 2013;20(11):1558–1568.
- [27] Gao L, Liu Y, Guo S, et al. Circulating long noncoding RNA HOTAIR is an essential mediator of acute myocardial infarction. *Cell Physiol Biochem*. 2017;44(4):1497–1508.
- [28] Redfors B, Shao Y, Omerovic E. Myocardial infarct size and area at risk assessment in mice. *Exp Clin Cardiol*. 2012;17(4):268–272.
- [29] Kim MY, Kim MJ, Yoon IS, et al. Diazoxide acts more as a PKC-epsilon activator, and indirectly activates the mitochondrial K(ATP) channel conferring cardioprotection against hypoxic injury. *Br J Pharmacol*. 2006;149(8):1059–1070.
- [30] Wang Y, Zhang X, Wei Z, et al. Platycodin D suppressed LPS-induced inflammatory response by activating LXRα in LPS-stimulated primary bovine mammary epithelial cells. *Eur J Pharmacol*. 2017;814:138–143.
- [31] Jiang LP, He CY, Zhu ZT. Role of microRNA-21 in radiosensitivity in non-small cell lung cancer cells by targeting PDCD4 gene. *Oncotarget*. 2017;8(14):23675–23689.
- [32] Wan N, Liu X, Zhang X-J, et al. Toll-interacting protein contributes to mortality following myocardial infarction through promoting inflammation and apoptosis. *Br J Pharmacol*. 2015;172(13):3383–3396.
- [33] Liu X, Wan N, Zhang X-J, et al. Vinexin-β exacerbates cardiac dysfunction post-myocardial infarction via mediating apoptotic and inflammatory responses. *Clin Sci (Lond)*. 2015;128(12):923–936.
- [34] Aydin S, Ugur K, Aydin S, et al. Biomarkers in acute myocardial infarction: current perspectives. *Vasc Health Risk Manag*. 2019;15:1–10.

- [35] Cheng S, Zhang X, Feng Q, et al. Astragaloside IV exerts angiogenesis and cardioprotection after myocardial infarction via regulating PTEN/PI3K/Akt signaling pathway. *Life Sci.* 2019;227:82–93.
- [36] Sun C, Jiang H, Sun Z, et al. Identification of long non-coding RNAs biomarkers for early diagnosis of myocardial infarction from the dysregulated coding-non-coding co-expression network. *Oncotarget.* 2016;7(45):73541–73551.
- [37] Cheng K, Zhao Z, Wang G, et al. lncRNA GAS5 inhibits colorectal cancer cell proliferation via the miR-182-5p/FOXO3a axis. *Oncol Rep.* 2018. DOI:10.3892/or.2018.6584.
- [38] Li S, Zhou J, Wang Z, et al. Long noncoding RNA GAS5 suppresses triple negative breast cancer progression through inhibition of proliferation and invasion by competitively binding miR-196a-5p. *Biomed Pharmacother.* 2018;104:451–457.
- [39] Wang M, Guo C, Wang L, et al. Long noncoding RNA GAS5 promotes bladder cancer cells apoptosis through inhibiting EZH2 transcription. *Cell Death Dis.* 2018;9(2):238.
- [40] Wang J, Gong X, Tian GG, et al. Long noncoding RNA growth arrest-specific 5 promotes proliferation and survival of female germline stem cells in vitro. *Gene.* 2018;653:14–21.
- [41] Rossé T, Olivier R, Monney L, et al. Bcl-2 prolongs cell survival after Bax-induced release of cytochrome c. *Nature.* 1998;391(6666):496–499.
- [42] Jürgensmeier JM, Xie Z, Deveraux Q, et al. Bax directly induces release of cytochrome c from isolated mitochondria. *Proc Natl Acad Sci U S A.* 1998;95(9):4997–5002.
- [43] Gustafsson AB, Gottlieb RA. Bcl-2 family members and apoptosis, taken to heart. *Am J Physiol Cell Physiol.* 2007;292(1):C45–51.
- [44] Gu GL, Xu X-L, Sun X-T, et al. Cardioprotective effect of MicroRNA-21 in murine myocardial infarction. *Cardiovasc Ther.* 2015;33(3):109–117.
- [45] Zhang H, Cai Y, Zheng L, et al. LncRNA BISPR promotes the progression of thyroid papillary carcinoma by regulating miR-21-5p. *Int J Immunopathol Pharmacol.* 2018;32:2058738418772652.
- [46] Liu X, She Y, Wu H, et al. Long non-coding RNA Gas5 regulates proliferation and apoptosis in HCS-2/8 cells and growth plate chondrocytes by controlling FGF1 expression via miR-21 regulation. *J Biomed Sci.* 2018;25(1):18.
- [47] Song J, Ahn C, Chun C-H, et al. A long non-coding RNA, GAS5, plays a critical role in the regulation of miR-21 during osteoarthritis. *J Orthop Res.* 2014;32(12):1628–1635.
- [48] Shen Z, She Q. Association between the deletion allele of ins/del polymorphism (Rs145204276) in the promoter region of GAS5 with the risk of atherosclerosis. *Cell Physiol Biochem.* 2018;49(4):1431–1443.
- [49] Pickard MR, Williams GT. Molecular and Cellular Mechanisms of Action of Tumour Suppressor GAS5 LncRNA. *Genes (Basel).* 2015;6(3):484–499.
- [50] Hu L, Ye H, Huang G, et al. Long noncoding RNA GAS5 suppresses the migration and invasion of hepatocellular carcinoma cells via miR-21. *Tumour Biol.* 2016;37(2):2691–2702.
- [51] Gui F, Hong Z, You Z, et al. MiR-21 inhibitor suppressed the progression of retinoblastoma via the modulation of PTEN/PI3K/AKT pathway. *Cell Biol Int.* 2016;40(12):1294–1302.
- [52] Li Y, Xia J, Jiang N, et al. Corin protects H<sub>2</sub>O<sub>2</sub>-induced apoptosis through PI3K/AKT and NF-κB pathway in cardiomyocytes. *Biomed Pharmacother.* 2018;97:594–599.
- [53] Wang K, Bei W-J, Liu Y-H, et al. miR-21 attenuates contrast-induced renal cell apoptosis by targeting PDCD4. *Mol Med Rep.* 2017;16(5):6757–6763.
- [54] Bai L, Liang R, Yang Y, et al. MicroRNA-21 regulates PI3K/Akt/mTOR signaling by targeting TGFβI during skeletal muscle development in pigs. *PLoS One.* 2015;10(5):e0119396.